Date: April 28, 2015
Refer to: LIGO-T1500202-v1

From: M. Zucker
To: LIGO Vacuum Review Board
cc: H. Overmier, K. Ryan, G. Moreno, J. Giaime, R. Oram, A. Lazzarini, D. Reitze
Re: **Optimization of beamtube pumping to mitigate acquired water vapor**

Abstract: Water vapor ingested from 2008 to 2012 appears to have increased the LLO Y tube's outgassing, slightly exceeding specified limits. A finite element diffusion model was used to assess resulting gas index phase noise. The model highlighted a historical oversight leading to systematic noise underestimation in situations with substantial conduction gradients, such as end-pumping of water vapor (the nominal default). The aLIGO configuration at LLO is especially vulnerable. A deployment of ion pumps is found to restore adequate noise margin.

Introduction: Length-averaged beamtube water vapor partial pressure was originally specified[1] as $<P(H_2O)>_L \leq 10^{-10}$ Torr. Measurements after each module bakeout indicated this would be feasible without distributed pumping.

With end-pumping only, average pressure is related to outgassing flux by

$$\langle P(H_2O)\rangle_L = Q\left(\frac{1}{12C_L}+\frac{1}{S}\right)$$

where $Q = JA$ is total outgassed current due to uniform flux J, A is the surface area (1.57×10^8 cm^2), C_L is the conductance for water vapor (58 l/s for 18 AMU and 4km at 293K), and S is total pumping speed ($S/2$ at each end). For $S \gg C_L$, this implies that we require outgassing flux $J(H_2O) \leq 4.4 \times 10^{-16}$ Tl/s/cm^2.

The LLO rodent-induced air leak at Y=2,258m admitted about 350 torr-liters of water vapor from October 2008 until it was sealed in December 2012, assuming 50% ambient relative humidity. In steady state, average internal partial pressure of water during the exposure would have been about 10^{-7} torr, assuming the vapor was conducted to the ends without immediate absorption.

The expected effect on future outgassing is not well constrained, due to the nonequilibrium state of the post-bake steel. Treating the related case of transient vapor from detector components streaming into the tube through the cryopumps, Weiss[2] predicts approximate reciprocity between exposure time t_0 at elevated pressure P_0, and recovery time t_1 to reach some goal pressure P_1. However this clearly breaks down unless $t_1 \gg t_0$, and therefore does not apply here. Indeed, for the present case the relation might be interpreted to suggest 4,000 years are needed to recover the goal pressure after 4 years at 1,000x higher pressure. This would be alarming, but it's clearly too pessimistic.

[1] M890001 table IV-D-1, p.49; for aLIGO, the original "goal" is now a "requirement"
[2] T080330 equation 2

A passive accumulation of about 100 hours was performed on this tube in November 2014, nominally to test for air leakage after repairs.[3] The residual gas analyzer at the midstation (Y=2,019m) recorded the water vapor partial pressure of 1.5×10^{-10} torr, 20 hours after the end gate valves were sealed. Since the relaxation time for water vapor is about 8 hours, we conservatively interpret this as if it was uniform a mean pressure, i.e., with pumping gradients relaxed.

The unpumped rate of rise measured thereafter would correspond to a uniform degassing flux of about 2.4×10^{-17} Tl/s/cm^2. However, the rate of rise is likely depressed due to surface redistribution, typical of water vapor after an abrupt change in pumping. The beginning pressure instead suggests a true asymptotic flux more like 6.6×10^{-16} Tl/s/cm^2. The tube wall temperature averaged 14C during this test; normalizing to 20C elevates the implied rate at standard temperature by about a factor of two.

Subsequent attempts[4] to measure water vapor in this location and at Y2-1 (Y=2,331m) have been limited by instrument backgrounds, and only constrain the peak partial pressure to $P(\max) < 1.6 \times 10^{-9}$ torr. Nevertheless, such limits, measured very near the original leak, confirm that the absorption/reemission model is far too pessimistic. More work is needed to model and understand persistent effects of vapor reexposure.

A finite element model was constructed to evaluate refractive index effects of the observed water vapor, and to plan installation of pumps to mitigate them. A uniform water outgassing rate of $J(H_2O)=1.3 \times 10^{-15}$ Tl/s/cm^2 was adopted for the simulation, based on the November 2014 measurement.

Method: The tube is approximated as 81 discrete nodes. Each is furnished a share of outgassing current and is joined to its neighbors by discrete conductances. Nodes corresponding to ends and to physical pump port locations[5] are optionally supplied with pumps. End nodes are each assigned 100,000 l/s effective speed, representing the LN_2 cryopumps. Ion pump nodes at designated port locations are each assigned the characteristic water vapor speed specified for a large commercial ion pump, derated for tubulation loss[6]. All pump speeds were presumed independent of pressure.

The nodes were initialized and then iteratively relaxed to balance influx, exhaust, and conduction with neighbors, until successive iterations differed by less than 0.5% everywhere.[7]

---

[3] T1400713

[4] LLO log entries # 17834 , 17827 , 16971

[5] D950031 sheet 3

[6] Gamma Vacuum model 1200LX DI (dual Ti/Ta elements); 534 l/s net, assuming 20 cm dia. x 20 cm connecting tube. Selecting all Ti elements could achieve 830 l/s net, at some increased risk of noble gas instability.

[7] 10^4 to 10^5 relaxations were required per case, depending on pump arrangement. The five cases presented here took a total of 3 seconds to converge on a 2.3 GHz Mac PowerBook Pro running Matlab R2014a.

Pressure profiles derived in this way for each pumping configuration were then integrated with the aLIGO arm cavity beam profile[8] according to P940008 eq. (1).[9] Five cases were evaluated:

1. No additional pumps, only the fixed cryopumps at vertex and end stations.
2. A single ion pump added at the midstation (MY).
3. Two ion pumps, one at MY and one at Y1-7 (next adjacent port toward the vertex). These straddle the location of the cavity beam waist.
4. Add to these two more at Y1-6 and Y2-1, the next available ports toward the vertex and end, respectively (four, centered over the beam waist).
5. All possible pumps, using every valve location (a total of 15 ion pumps, in addition to the two fixed cryopumps).

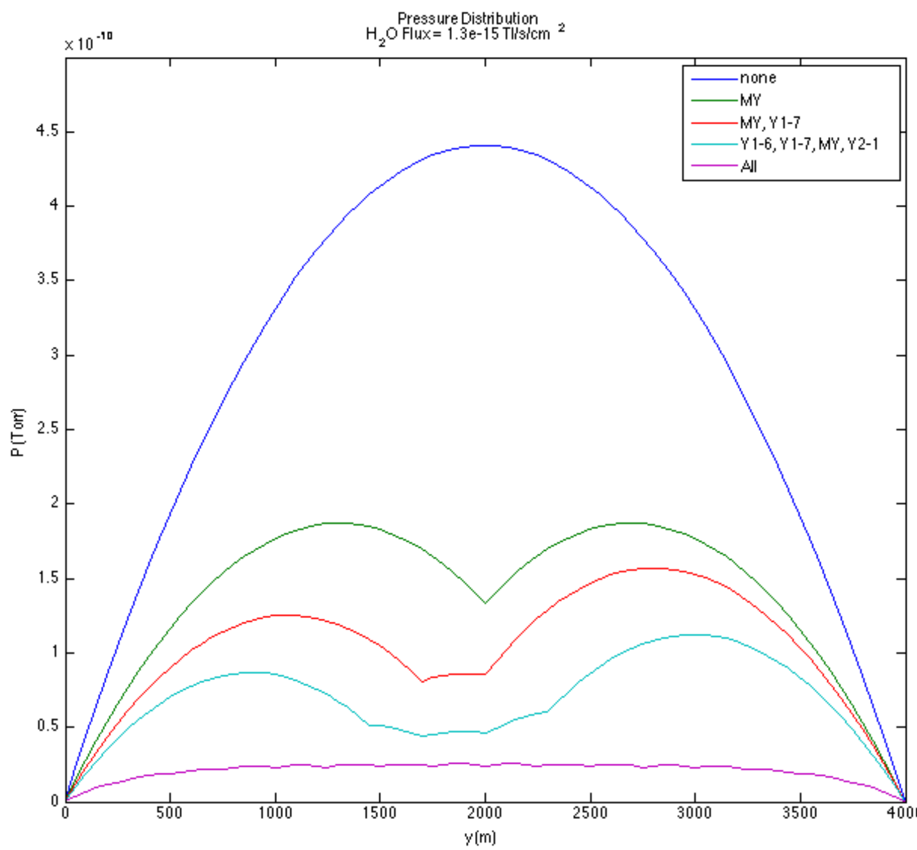

Figure 1: Pressure profiles for five ion pump arrangements with *J(H₂0)* = 1.3 x10^{-15} Tl/s/cm^2.

[8] P1400177

[9] Modified to bring molecular number density ρ inside the integral.

Results: Pressure profiles are shown in Figure 1. As a check, limiting cases 1 and 5 are seen to match their corresponding analytical expressions. The mean and peak pressures and phase noise integrals are summarized in Table 1 and Figure 2.

Substituting molecular constants for hydrogen recovers the accepted LIGO strain noise result closely. However, reinstating the appropriate mass and refractive index for water vapor gives a factor of 4.2 higher strain noise than calculated for hydrogen in the end-pumped condition (case 1). Prior treatments[10] typically report $\tilde{h}(H_2O) = 3.3\,\tilde{h}(H_2)$.

The prior scalings for heavier species were based on local optical effects of molecular polarizability and thermal velocity. The present calculation includes an additional implicit mass (velocity) dependence, due to density gradients along the tube. Previously neglected, this is more pronounced with heavier species; its effect is enhanced by the sharply focused aLIGO cavity geometry. The discrepancy is less for uniform pressure profiles and lighter molecules, as expected. To help illustrate the issue, Figure 3 shows the beam radius plotted with the phase noise integrands for each case.

Ion Pumps Deployed	*Mean P (10^{-10} Torr)*	*Peak P (10^{-10} Torr)*	*Strain (10^{-25} $Hz^{-1/2}$)*	*Norm. Strain*
none	2.91	4.41	3.10	≡1.00
MY	1.39	1.87	2.06	0.66
MY, Y1-7	1.03	1.57	1.72	0.55
Y1-6, Y1-7, MY, Y2-1	0.69	1.12	1.35	0.44
all	0.21	0.25	0.79	0.25

Table 1: Mean and peak water vapor pressure and strain noise contribution (one arm) for each pumping arrangement, assuming uniform *J*(H_20) = 1.3x10^{-15} Tl/s/cm^2.

[10] e.g., M890001 , G950082 or G1300116

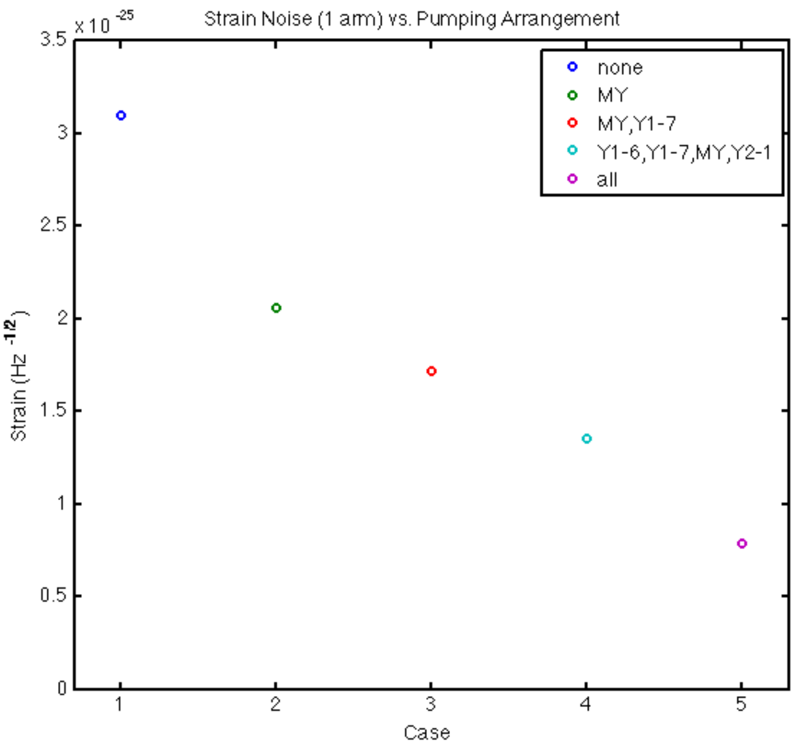

Figure 2: Strain noise PSD (one arm) for each pumping configuration.

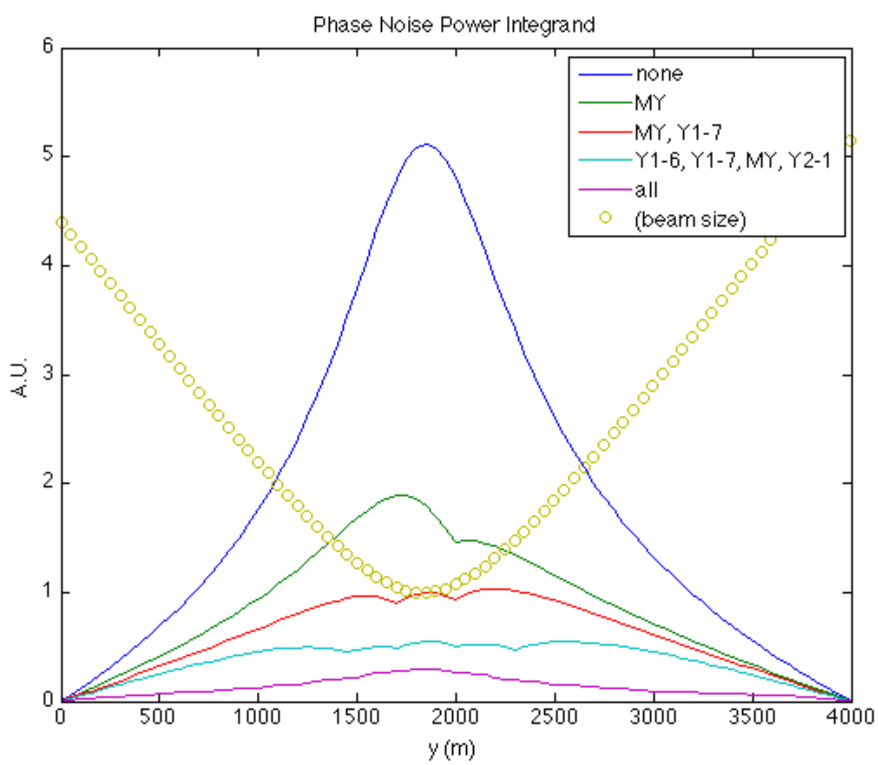

Figure 3: Phase noise PSD integrand.

Discussion: The lowest point in the best proposed aLIGO sensitivity curve of T1400177 reaches $\tilde{h}(f) = 2.6 \times 10^{-24}/\sqrt{Hz}$ (Fig. 3, "BNS optimized," 125 W input, 250 Hz). The calculated phase noise is less than 1/10 this level[11] with one added pump at the midpoint (Table 1, case 2). The default case 1, no added pumps, may in fact become adequate by itself: outgassing is expected to decline as ~1/*t*, and this performance level is unlikely to be achieved until the time since the leak repair has at least doubled.

On the other hand, as discussed earlier, determining the residual water vapor pressure has proven difficult and uncertain. The presumed source rate used here is based on a single measurement, and we have no proven model to fall back on.

If we pessimistically take the 1.6×10^{-9} torr Y2-1 upper limit measured in April 2015 (with end pumping active) as a "worst-case" estimate of peak (central) water vapor pressure, implying an effective mean pressure 1.1×10^{-9} torr, the corresponding outgassing flux is 4.8×10^{-15} Tl/s/cm^2. In this instance, case 4 (four pumps) just brings the phase noise to 1/10 the minimum of $\tilde{h}(f)$.

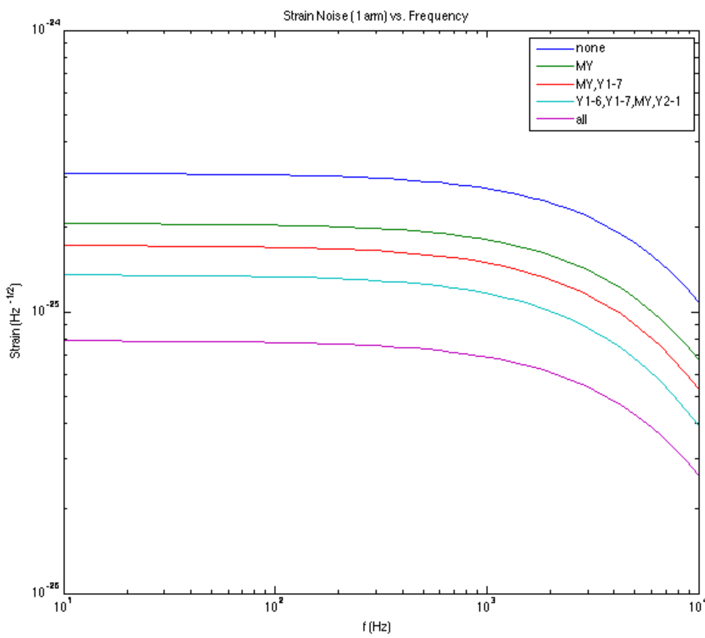

Figure 4: Strain noise frequency dependence.

Appendix: Frequency response. Since the closest approach to the ultimate strain envelope occurs at the "high" frequency of 250 Hz, and frequency response is also affected by beam radius, it was worth double-checking. As shown in Figure 4, the index fluctuation noise at 250 Hz is within 3% of the DC asymptote for water vapor. Frequency response was thus neglected in the calculations cited above.

---

[11] our customary margin for "technical" noise terms.